Electron localization in linear chains of identical loop scatterers

Chih-Lung Chou*
Department of Physics, Chung Yuan Christian University,
Taoyuan 32023, Taiwan and
Department of Science Education,
Taipei Municipal University of Education,
Taipei 10048, Taiwan
(Dated: February 6, 2008)

We show that electron localization is generic in a linear chain of identical simple quantum wire loops with equal arm lengths in the presence of either a perpendicular magnetic field or the spin-orbit interaction, and has less to do with the shapes of the loops. We calculate the transfer matrices for a general simple loop scatterer in the presence of these effects. Based on the knowledge of the transfer matrices, we thus provide a criterion for the occurrence of the localization and present a simple formalism to integrate the transmission probability over the injection wave vector of electron.

I. INTRODUCTION

It has been shown that electron localization can be induced by magnetic field in particular class of two dimensional quantum network called the $\mathcal{T}_3$ network[1]. The localization is due to the interplay of the network geometry and the Aharonov-Bohm effect[2]. In this case, electrons travelling in the network will acquire quantum phases due to the Aharonov-Bohm effect. For specific values of the magnetic field, totally destructive interference occurs and the electron motion is confined in a small portion of the network that is called AB cage. In experiment the onset of electron localization in a quantum network is usually detected by transport measurement. This localization phenomenon has been experimentally observed in superconduction $\mathcal{T}_3$ network[3] and in two-dimensional normal metal networks[4]. Different aspects of AB cages such as the effect of disorder[5], interaction induced delocalization[6], and transport[7] are also discussed in literature. Electron localization is also predicted in a linear chain of square loops connected at one vertex in the presence of the spin-orbit interaction called the Rashba SO coupling[8,9]. Similarly, the localization is due to the interplay of the network geometry and the Aharonov-Casher effect[10]. In this case, electrons travelling in the network will acquire quantum phases due to the Aharonov-Casher effect. For specific values of the spin-orbit coupling strength, electrons are forbidden to transport in the chain and the averaged conductance becomes zero.

In this paper we discuss when and why the electron localization phenomenon occurs in a linear chain of N identical scatterers in the large N limit. If the scatterers are quantum wire loops, will the shape of the loops matter in the occurrence of the localization phenomenon? To answer these questions, we first review the parametrization of the transfer matrix for a single scatterer with a single input lead and a single output lead connected to the scatterer. The electron transmission probability for a linear chain of the scatterers can be easily obtained from the elements of the transfer matrix. Typically, the transmission probability reveals a binary behavior. In some domains of the parameters that parameterize transfer matrix, the transmission probability vanishes in the large N limit. In the other domains of the parameters, the transmission probability is relatively high and oscillates rapidly. In real situation, the binary structure of electron transmission may be determined by the factors such as the injection electron wave vector k, the geometry of the scatterer, and other physical effects such as magnetic field and spin-orbit interaction, et.c. It is possible that zero electron transmission always occurs in some linear chains of scatterers no matter what the value of k is. In this case, electron localization is seen as zero transmission in the averaged transmission probability after integrating over the injection wave vector k.

The paper is organized as follows. In section II, we review the parametrization of the transfer matrix for a spin-blind scatterer with an input lead and an output lead connected to it. The transfer matrix is known to respect $U(1,1)$ symmetry. We then discuss the transmission probability for the linear chain of the scatterers and express the probability in terms of the parameters that parameterize the transfer matrix. We also define a criterion function for determining whether the electron transmission is forbidden in the chain of scatterers. We show that the criterion function can be easily read off from the transfer matrix of a single scatterer. On the other hand, a typical spin-sensitive scatterer may respect a larger symmetry, the $U(2,2)$ symmetry. In some cases, however, the transfer matrix of a spin-sensitive scatterer is factorized into the spatial part and the spin part, and respects $U(1,1) \otimes U(2)$ symmetry. Here $U(1,1)$ is the symmetry for the spatial part of the transfer matrix and $U(2)$ is the symmetry for the spin part of the transfer matrix. In these cases, the total transmission probability is only determined by the spatial part of the transfer matrix. In section III, we study simple loop scatterers of arbitrary shapes in the presence of either magnetic field or the spin-orbit interaction. We derive the transfer matrices for the loops and discuss the onset of electron

localization in the linear chains of the loops. As examples, we discuss the circular loop scatterers, the square loop scatterers, and the triangular loop scatterers in details along with their transfer matrices. Throughout the paper, we assume that the loops and the leads are made by single-channel quantum wires for simplicity. The presence or the absence of electron localization in the loop chains is shown to be easily known from the criterion functions of the loop scatterers. In section IV, we present a simple formalism for integrating the transmission probability over k. The averaged transmission probabilities for the loop chains discussed in the paper are calculated in this section. In section V, we give our conclusion.

II.   SCATTERERS WITH AN INPUT LEAD AND AN OUTPUT LEAD

A.   Transfer matrix for spin-blind scatterers

In this section we describe the transfer matrix for an arbitrary spin-blind scatterer with only an input lead and an output lead connected to it. Consider a scatterer as shown in Fig.1. The dark circle represents the unknown scatterer. Two single-channel quantum wires are connected to the scatterer such that electrons can move in the wires and tunnel through the scatterer. By assuming that electrons move as free particles in the wires, the electron wave functions on the two leads are written as $\psi_I(x) = A_I e^{ikx} + B_I e^{-ikx}$ and $\psi_{II}(x') = A_{II} e^{ikx'} + B_{II} e^{-ikx'}$, respectively. Here k denotes the injection wave vector for electrons, x and x' denote the coordinates on the leads, and the constants A_I, B_I, A_{II}, B_{II} are the amplitudes of the waves. The conservation of electron current then implies that $|A_I|^2 - |B_I|^2 = |A_{II}|^2 - |B_{II}|^2$. In general, quantum mechanics also implies the following linear relation between the amplitudes

$$
\begin{pmatrix} A_{II} \\ B_{II} \end{pmatrix} = T \begin{pmatrix} A_I \\ B_I \end{pmatrix},
\tag{1}
$$

where T is called the transfer matrix for the scatterer. It is obvious that T is an element of $U(1,1)$ group. The most general form of T can be parameterized as

$$
T = e^{i\alpha} \begin{pmatrix} e^{i\beta}\cosh\theta & e^{-i\gamma}\sinh\theta \\ e^{i\gamma}\sinh\theta & e^{-i\beta}\cosh\theta \end{pmatrix},
\tag{2}
$$

where α, β, θ, and γ are the introduced parameters to be determined by the nature of the scatterer and the injection wave vector of electrons.

With the parameterized T given in Eq.(2), we find the eigenvalues $\lambda_\pm$ and the corresponding eigenvectors $\vec{\phi}_\pm$ as follows:

$$
\lambda_\pm = e^{i\alpha}(\cosh\theta\cos\beta \pm \sqrt{(\cosh\theta\cos\beta)^2 - 1})
\tag{3}
$$

$$
\vec{\phi}_\pm = (\cosh\theta\sin\beta \mp i\sqrt{(\cosh\theta\cos\beta)^2 - 1}, -ie^{i\gamma}\sinh\theta).
\tag{4}
$$

The transfer matrix T is then diagonalized with the help of the 2×2 matrix Λ

$$
T_D \equiv \begin{pmatrix} \lambda_+ & 0 \\ 0 & \lambda_- \end{pmatrix} = \Lambda^{-1} T \Lambda,
\tag{5}
$$

where the first and the second columns of Λ are the eigenvectors $\vec{\phi}_+$ and $\vec{\phi}_-$, respectively.

B.   Chain of identical spin-blind scatterers

Consider a linear chain of N identical spin-blind scatterers as shown in Fig.2. The electronic wave amplitudes at the two ends of the chain are related by

$$
\begin{pmatrix} A_N \\ B_N \end{pmatrix} = \Lambda T_D^N \Lambda^{-1} \begin{pmatrix} A_0 \\ B_0 \end{pmatrix}.
\tag{6}
$$

Now let M denote the transformation matrix $M \equiv \Lambda T_D^N \Lambda^{-1}$. Suppose that an electron is injected from the left end of the chain. The electron will tunnel through the chain of scatterers with the tunnelling amplitude t, or be reflected

by the scatterers with the reflection amplitude r,

$$t = \frac{\det M}{M_{22}} = \frac{e^{i2N\alpha}}{M_{22}}, \tag{7}$$

$$r = \frac{-M_{21}}{M_{22}}. \tag{8}$$

Here M_{ij} denote the entries of M

$$M_{21} = \frac{e^{i\gamma}(\lambda_+^N - \lambda_-^N)\sinh\theta}{2\sqrt{(\cosh\theta\cos\beta)^2 - 1}}, \tag{9}$$

$$M_{22} = \frac{\lambda_+^N + \lambda_-^N}{2} - i\frac{(\lambda_+^N - \lambda_-^N)\cosh\theta\sin\beta}{2\sqrt{(\cosh\theta\cos\beta)^2 - 1}}. \tag{10}$$

As the number of scatterers N becomes large, the electronic transmission will be highly suppressed for $(\cosh\theta\cos\beta)^2 > 1$. In this low transmission scenario, the transmission probability is roughly

$$|t|^2 \simeq \frac{4[(\cosh\theta\cos\beta)^2 - 1]}{|\lambda|^{2N}\sinh^2\theta}, \tag{11}$$

where $|\lambda| = \max(|\lambda_+|, |\lambda_-|)$ is the larger one of the absolute values of the two eigenvalues. The electronic transmission will finally be turned off as N goes to infinity. For $(\cosh\theta\cos\beta)^2 < 1$, the eigenvalues can be written as $\lambda_\pm = e^{i(\alpha\pm\Omega)}$ with $\Omega \equiv \cos^{-1}(\cosh\theta\cos\beta)$. In this scenario the electronic transmission is high and the transmission probability is found as exactly

$$|t|^2 = \frac{\sin^2\Omega}{\sin^2\Omega + \sinh^2\theta\sin^2(N\Omega)}. \tag{12}$$

Obviously, the transmission probability oscillates rapidly in Ω for large N. In the large N limit, the averaged transmission probability over the small interval $[\Omega, \Omega + 2\pi/N]$ is

$$|t|^2 = \frac{|\sin\Omega|}{\sqrt{\sin^2\Omega + \sinh^2\theta}}. \tag{13}$$

Finally, the transmission probability becomes unity when $(\cosh\theta\cos\beta)^2 = 1$.

Based upon the above discussion, the value of $(\cosh\theta\cos\beta)^2$ is critical in determining the characteristics of the electronic transmission in a chain of spin-blind scatterers. In real situation, $(\cosh\theta\cos\beta)^2$ is a function of several dynamical and geometrical factors of the scatterer. In the remaining parts of the paper, we call the function as the criterion function for electronic transmission. For examples, the injection wave vector k, the Aharonov-Bohm flux Φ_{AB}, and the ring radius a together will determine the $(\cosh\theta\cos\beta)^2$ value of the equal-arm ring scatterer in the presence of a perpendicular magnetic field[11]

$$(\cosh\theta\cos\beta)^2 = \frac{\cos^2(\pi ka)}{\cos^2(\Phi_{AB}/2)}. \tag{14}$$

As long as ka is not a half-integer, the low electronic transmission condition $(\cosh\theta\cos\beta)^2 > 1$ is always held when $\Phi_{AB} = (2n+1)\pi$ for integers n. Extremely low transmission still survives even if we integrate the transmission probability over k. Therefore electron localization occurs in the chain of equal-arm rings in the presence of a perpendicular magnetic field.

C. Spin-sensitive scatterers

In this subsection we briefly discuss spin-sensitive scatterers. Once again, the scatterer is connected to two leads as shown in Fig.1. The wave functions in the leads I and II are written as $\psi_I(x) = A_I e^{ikx}\chi_I + B_I e^{-ikx}\eta_I$ and $\psi_{II}(x') = A_{II}e^{ikx'}\chi_{II} + B_{II}e^{-ikx'}\eta_{II}$. Here $\chi_I, \chi_{II}, \eta_I$ and η_{II} are normalized spinors, A_I, A_{II}, B_I and B_{II} are amplitudes of the waves. In general, $A_{II}, B_{II}, \chi_{II}$ and η_{II} can be viewed as functions of A_I, B_I, χ_I and η_I. If we write the electron current fluxes into the spin-up and the spin-down parts by $|A_i|^2 = |A_i^\uparrow|^2 + |A_i^\downarrow|^2$ and $|B_i|^2 = |B_i^\uparrow|^2 + |B_i^\downarrow|^2$,

then the current conservation gives $|A_I^\uparrow|^2 + |A_I^\downarrow|^2 - |B_I^\uparrow|^2 - |B_I^\downarrow|^2 = |A_{II}^\uparrow|^2 + |A_{II}^\downarrow|^2 - |B_{II}^\uparrow|^2 - |B_{II}^\downarrow|^2$. As easily seen from the equation, the transfer matrix for the spin-sensitive scatterer must respect $U(2,2)$ symmetry.

In some cases, the symmetry for the transfer matrix is smaller. For example, the symmetry is $T \otimes S$ for the ring-shape and the diamond-shape scatterers with Rashba spin-orbit coupling[8,9,11]. Here T is an element of $U(1,1)$ group and acts on the spatial part of the electron wave function as in Eq.(1), while S denotes an element of $U(2)$ group and acts on the spin part of the electron wave functions, $\chi_{II} = S\chi_I$ and $\eta_{II} = S\eta_I$. Obviously, the total electronic transmission probability is merely determined by T and has nothing to do with the spin-part symmetry S. In these cases, the spin-sensitive scatterers are effectively spin-blind in discussing their total transmission probabilities.

III. QUANTUM WIRE LOOPS AS SCATTERERS

In this section, we first discuss simple loop scatterers in the presence of either a perpendicular magnetic field or the spin-orbit interaction. We derive the transfer matrices for the loop scatterers. It is found that the transfer matrices merely depend on the injection wave vector k, the arm lengths of the loops, and the Aharonov-Bohm phases or the spin-orbit coupling strength. We then apply our results to the linear chains of the circular loops[11], the square loops[8,9] and the triangular loops. We take all these quantum wire loops as scatterers and find their transfer matrices. Given the transfer matrices, we thus obtain the criterion function $(\cosh\theta\cos\beta)^2$ as well as the parameter $\sinh\theta$ that appears in the parameterized transfer matrix in Eq.(2).

A. Simple loops in the presence of a perpendicular magnetic field

Consider the scatterer that is made by a simple quantum wire loop with two leads in the presence of a perpendicular magnetic field as shown in Fig.3. The simple loop can be of any shapes. Let r_1 and r_2 denote the path lengths measured from the node 1 along the upper arm and the lower arm, respectively. The total length of the upper arm of the loop is L_1 while the total length of the lower arm is L_2. In general, the two arm lengths may not be equal to each other.

Suppose that an electron is injected into the loop with energy $\varepsilon = \hbar^2 k^2/2m$, then the electron wave functions in the two leads and in the loop arms are given by

$$\psi_I(x) = A_I e^{ikx} + B_I e^{-ikx}, \tag{15}$$

$$\psi_{II}(x) = A_{II} e^{ikx'} + B_{II} e^{-ikx'}, \tag{16}$$

$$\psi_{up}(r_1) = e^{i\frac{e}{\hbar}\int_0^{r_1} \vec{A}\cdot d\vec{r}_1}(a_1 e^{ikr_1} + b_1 e^{-ikr_1}), \tag{17}$$

$$\psi_{low}(r_2) = e^{i\frac{e}{\hbar}\int_0^{r_2} \vec{A}\cdot d\vec{r}_2}(a_2 e^{ikr_2} + b_2 e^{-ikr_2}), \tag{18}$$

where k is the injection wave vector, e is the electric charge for electrons, m denotes the effective mass for electrons , $\vec{A}$ denotes the vector potential for the magnetic field, and x and x' are the coordinates on the leads that are measured from the node 1 and the node 2, respectively. Here ψ_{up} is the wave function in the upper arm and ψ_{low} denotes the wave function in the lower arm. The coefficients A_I, B_I, A_{II}, B_{II} and a_i, b_i are the amplitudes of the electronic waves. By considering the continuity of wave function and the current conservation at the junctions, we get the transfer matrix for the loop scatterer

$$\begin{pmatrix} A_{II} \\ B_{II} \end{pmatrix} = e^{i(\frac{\Phi_1+\Phi_2}{2}-\Theta_{AB})}\begin{pmatrix} t_2 & -it_1 \\ it_1 & t_2^* \end{pmatrix}\begin{pmatrix} A_I \\ B_I \end{pmatrix}, \tag{19}$$

with

$$\Theta_{AB} = \arctan[(\frac{\sin\theta_1 - \sin\theta_2}{\sin\theta_1 + \sin\theta_2})\tan(\frac{\Phi_{AB}}{2})], \tag{20}$$

$$t_2 = \frac{4\sin(\theta_1+\theta_2) + i[\cos(\theta_1-\theta_2) - 5\cos(\theta_1+\theta_2) + 4\cos(\Phi_{AB})]}{4\sqrt{\sin^2\theta_1 + \sin^2\theta_2 + 2\sin\theta_1\sin\theta_2\cos(\Phi_{AB})}}, \tag{21}$$

$$t_1 = \frac{\cos(\theta_1-\theta_2) + 3\cos(\theta_1+\theta_2) - 4\cos(\Phi_{AB})}{4\sqrt{\sin^2\theta_1 + \sin^2\theta_2 + 2\sin\theta_1\sin\theta_2\cos(\Phi_{AB})}}. \tag{22}$$

Here t_2^* is the complex conjugate of t_2, and Φ_1 and Φ_2 are the Aharonov-Bohm phases acquired by the electrons travelling in the upper arm and the lower arm, respectively. $\Phi_{AB} \equiv \Phi_1 - \Phi_2$ is the Aharonov-Bohm flux of the

loop, and the phases are defined as $\theta_1 \equiv kL_1$ and $\theta_2 \equiv kL_2$. Comparing Eq.(19) to (2), we find the transfer matrix parameter $\sinh\theta = t_1$ and the criterion function

$$(\cos\beta\cosh\theta)^2 = \frac{\sin^2(\theta_1+\theta_2)}{\sin^2\theta_1 + \sin^2\theta_2 + 2\sin\theta_1\sin\theta_2\cos(\Phi_{AB})}. \tag{23}$$

Eq.(23) shows that the low electronic transmission condition $(\cos\beta\cosh\theta)^2 > 1$ cannot be always satisfied for all k values unless for $L_1 = L_2$. When $L_1 = L_2 = L$, the criterion function becomes $(\cos\beta\cosh\theta)^2 = \cos^2(kL)/\cos^2(\Phi_{AB}/2)$. For the equal-arm loop chains in the presence of a perpendicular magnetic field, electron localization will occur at $\Phi_{AB} = (2n+1)\pi$ for all integers n.

B. Simple loop with spin-orbit interaction

Consider a general loop scatterer with spin-orbit interaction as shown in Fig.3. In general, the upper arm of the loop can be viewed as being made by N_1 linking bonds connected in series. The lower arm is viewed as being made by N_2 linking bonds connected in series. Typically, the numbers of bonds N_1 and N_2 could be very large. Let r_{1p} and r_{2p} denote the coordinates of the p-th linking bonds for the upper arm and the lower arm, respectively. The beginning of the p-th linking bonds for the arms are labelled as $r_{1p} = 0$ and $r_{2p} = 0$, while the ends of the bonds are labelled as $r_{1p} = \ell_{1p}$ and $r_{2p} = \ell_{2p}$. The Hamiltonian H_{ip} ($i=1,2$) for an electron moving in the p-th linking bonds in the upper arm or the lower arm is given by

$$H_{ip} = -\frac{\hbar^2}{2m}[\frac{\partial}{\partial r_{ip}} - ik_{so}(\vec{\sigma}\cdot(\hat{z}\times\hat{r}_{ip}))]^2 - \frac{\hbar^2 k_{so}^2}{2m}, \quad i=1,2. \tag{24}$$

where k_{so} is the coupling strength for spin-orbit interaction, m is the effective mass of electron, $\hat{z}$ is the unit direction normal to the loop, and $\hat{r}_{ip}$ is the unit direction along the p-th linking bonds in the arms. The wave function $\psi_{up}(r_{1p})$ with the energy $\varepsilon = \hbar^2 k^2/2m$ in the upper arm is thus obtained by

$$\psi_{up}(r_{1p}) = e^{ik_{so}r_{1p}(\vec{\sigma}\cdot(\hat{z}\times\hat{r}_{1p}))}S_{p-1}^{(1)}S_{p-2}^{(1)}\cdots S_1^{(1)}[a_1 e^{iqr_1} + b_1 e^{-iqr_1}], \tag{25}$$

where a_1 and b_1 are constant spinors, k is the injection wave vector, $q \equiv \sqrt{k^2 + k_{so}^2}$ is the wave vector for the electrons moving in the arms of the loop, $r_1 = r_{1p} + \sum_{n=1}^{p-1}\ell_{1n}$ is the path length measured from the node 1 to the position r_{1p}, and the spin-rotation operators $S_n^{(1)}$ are defined as $S_n^{(1)} \equiv e^{ik_{so}\ell_{1n}(\vec{\sigma}\cdot(\hat{z}\times\hat{r}_{1n}))}$. Similarly, the wave function in the lower arm of the loop is given by

$$\psi_{low}(r_{2p}) = e^{ik_{so}r_{2p}(\vec{\sigma}\cdot(\hat{z}\times\hat{r}_{2p}))}S_{p-1}^{(2)}S_{p-2}^{(2)}\cdots S_1^{(2)}[a_2 e^{iqr_2} + b_2 e^{-iqr_2}], \tag{26}$$

where a_2 and b_2 are constant spinors, $r_2 = r_{2p} + \sum_{n=1}^{p-1}\ell_{2n}$ is the path length measured from the node 1 to the position r_{2p}, and the spin-rotation operators $S_n^{(2)}$ are defined as $S_n^{(2)} \equiv e^{ik_{so}\ell_{2n}(\vec{\sigma}\cdot(\hat{z}\times\hat{r}_{2n}))}$. At the node 2, the wave functions in the arms become

$$\psi_{up}(r_1 = L_1) = S_1[a_1 e^{iqL_1} + b_1 e^{-iqL_1}], \tag{27}$$
$$\psi_{low}(r_2 = L_2) = S_2[a_2 e^{iqL_2} + b_2 e^{-iqL_2}], \tag{28}$$

where S_1 is the total spin-rotation operator for the upper arm and S_2 is the total spin-rotation operator for the lower arm,

$$S_1 \equiv S_{N_1}^{(1)}S_{N_1-1}^{(1)}\cdots S_1^{(1)}, \tag{29}$$
$$S_2 \equiv S_{N_2}^{(2)}S_{N_2-1}^{(2)}\cdots S_1^{(2)}. \tag{30}$$

Here L_1 and L_2 denote the arm lengths of the upper arm and the lower arm, respectively.
On the other hand, the wave functions in the leads are given by

$$\psi_I(x) = A_I e^{ikx} + B_I e^{-ikx}, \tag{31}$$
$$\psi_{II}(x') = A_{II} e^{ikx'} + B_{II} e^{-ikx'}. \tag{32}$$

Here x is the coordinate on the input lead with $x = 0$ being at the node 1, and x' is the coordinate on the output lead with $x' = 0$ being at the node 2. The spinor amplitudes A_{II} and B_{II} are connected to the A_I and B_I through the continuity of wave function and current conservation at the nodes 1 and 2. The continuity of wave function at the nodes 1 and 2 gives

$$A_I + B_I \; = \; a_1 + b_1 = a_2 + b_2, \tag{33}$$
$$A_{II} + B_{II} \; = \; S_1(a_1 e^{iqL_1} + b_1 e^{-iqL_1}) = S_2(a_2 e^{iqL_2} + b_2 e^{-iqL_2}). \tag{34}$$

Current conservation at the nodes leads to the Griffith's boundary conditions as follows

$$\frac{k}{q}(A_I - B_I) \; = \; a_1 - b_1 + a_2 - b_2, \tag{35}$$

$$\frac{k}{q}(A_{II} - B_{II}) \; = \; S_1(a_1 e^{iqL_1} - b_1 e^{-iqL_1}) + S_2(a_2 e^{iqL_2} - b_2 e^{-iqL_2}). \tag{36}$$

Solving the equations in the above, we get the transformation

$$\begin{pmatrix} A_{II} \\ B_{II} \end{pmatrix} = \begin{pmatrix} t_2 & -it_1 \\ it_1 & t_2^* \end{pmatrix} \begin{pmatrix} S(k_{so}, q) A_I \\ S(k_{so}, q) B_I \end{pmatrix}. \tag{37}$$

Here the 2×2 unitary matrix $S(k_{so}, q)$ is the transfer matrix in spin dimension and is defined as

$$S(k_{so}, q) = \frac{1}{\sqrt{f(k_{so}, q)}}[S_1 + \frac{\sin(\theta_1)}{\sin(\theta_2)} S_2], \tag{38}$$

with $\theta_1 \equiv qL_1$ and $\theta_2 \equiv qL_2$, and

$$f(k_{so}, q) \equiv 1 + \frac{\sin^2(\theta_1)}{\sin^2(\theta_2)} + 2\cos(\Theta_{so})\frac{\sin(\theta_1)}{\sin(\theta_2)}, \tag{39}$$

where $\cos(\Theta_{so}) \equiv \frac{1}{4}\mathrm{Tr}(S_2 S_1^{-1} + S_1 S_2^{-1})$ is a function of k_{so}. It is noted that $S_2 S_1^{-1} + S_1 S_2^{-1} = 2\cos(\Theta_{so})\mathbb{I}_2$, where $\mathbb{I}_2$ denotes the 2×2 identity matrix. The matrix elements in Eq.(37) are obtained by

$$t_2 \; = \; \frac{\sin(\theta_1 + \theta_2)}{\sin(\theta_2)\sqrt{f(k_{so}, q)}} + i\{\frac{k^2 \sin^2(\theta_1) + q^2[f(k_{so}, q) - \csc^2(\theta_2)\sin^2(\theta_1 + \theta_2)]}{2kq\sin(\theta_1)\sqrt{f(k_{so}, q)}}\}, \tag{40}$$

$$t_1 \; = \; \frac{k^2 \sin^2(\theta_1) - q^2[f(k_{so}, q) - \csc^2(\theta_2)\sin^2(\theta_1 + \theta_2)]}{2kq\sin(\theta_1)\sqrt{f(k_{so}, q)}}. \tag{41}$$

Obviously, the transfer matrix in Eq.(37) is of the type $T \otimes S$ and the total electronic transmission is merely determined by the matrix elements of T. The parameter $\sinh\theta$ in Eq.(2) is equal to t_1 in Eq.(41), and the criterion function for the chain of loops is found by

$$(\cosh\theta \cos\beta)^2 = \frac{\sin^2(\theta_1 + \theta_2)}{\sin^2(\theta_2)f(k_{so}, q)}. \tag{42}$$

In Eq.(42), the variables k_{so} and q are not separated generically. When $L_1 = L_2$ both S and f become functions of k_{so}, $S(k_{so}) = \frac{1}{\sqrt{f(k_{so})}}(S_1 + S_2)$ and $f(k_{so}) = 2(1 + \cos(\Theta_{so}))$, so that k_{so} and q are separated in Eq.(42). In the equal-arm case, the criterion function is always larger than 1 for some specific values of k_{so} that satisfy $f(k_{so}) = 0$, i.e, $\cos(\Theta_{so}) = -1$. Therefore, electron localization occurs naturally in the equal-arm loop chains with spin-orbit interaction.

C.   Circular Loops with spin-orbit interaction

Assume that an electron with energy $\varepsilon = \hbar^2 k^2/2m$ is injected into the linear chain of circular loops as shown in Fig.4. The radius of the rings is denoted as a. Both the lengths of the upper arm and the lower arm are equal to each other and are denoted as $L_1 = L_2 = \pi a$. As discussed in literature[11], the transfer matrix and the electronic transmission are obtained for the equal-arm ring scatterer in the presence of the spin-orbit interaction. Here we

derive the transfer matrix again by using the results obtained in the previous subsections. It is found that electron localization will occur in the chain of rings with the spin-orbit interaction.

The transfer matrix is given in Eq.(37). To know the exact form of the transfer matrix, we need the total spin-rotation operators S_1 and S_2 for the upper arms and lower arms of the ring, respectively. Here we derive the total spin-rotation operators as follows. Let φ_1 be the angles on the upper arm measured from the the node 1, and φ_2 denote the angle on the lower arm that is also measured from the node 1 as shown in Fig.5. From Eq.(25), the electron wave function Ψ_{up} in the upper arm is given by $\psi_{up}(\varphi_1) = S_1(\varphi_1)[a_1 e^{iqa\varphi_1} + b_1 e^{-iqa\varphi_1}]$. We then find the differential equation for the spin-rotation operator $S_1(\varphi_1)$ as

$$\frac{dS_1}{d\varphi_1} = i\theta_{so}\sigma_r(\varphi_1)S_1(\varphi_1), \tag{43}$$

where $\theta_{so} \equiv k_{so}a$, and σ_r is defined as $\sigma_r(\varphi_1) \equiv [-\cos(\varphi_1)\sigma_1 + \sin(\varphi_1)\sigma_2]$. By considering that the unitary operator $S_1(\varphi_1)$ is equal to the identity operator at $\varphi_1 = 0$, we obtain $S_1(\varphi_1)$ as

$$S_1(\varphi_1) = \frac{1}{1+\rho^2} \begin{pmatrix} e^{-i\lambda_1\varphi_1} + \rho^2 e^{i\lambda_2\varphi_1} & \rho[e^{-i\lambda_1\varphi_1} - e^{i\lambda_2\varphi_1}] \\ \rho[e^{-i\lambda_2\varphi_1} - e^{i\lambda_1\varphi_1}] & e^{i\lambda_1\varphi_1} + \rho^2 e^{-i\lambda_2\varphi_1} \end{pmatrix}, \tag{44}$$

where $\rho = (\theta_{so}/\lambda_2)$, $\lambda_1 = (\sqrt{1+4\theta_{so}^2} - 1)/2$, and $\lambda_2 = (\lambda_1 + 1)$. Similarly, we obtain $S_2(\varphi_2)$ as

$$S_2(\varphi_2) = \frac{1}{1+\rho^2} \begin{pmatrix} e^{i\lambda_1\varphi_2} + \rho^2 e^{-i\lambda_2\varphi_2} & \rho[e^{i\lambda_1\varphi_2} - e^{-i\lambda_2\varphi_2}] \\ \rho[e^{i\lambda_2\varphi_2} - e^{-i\lambda_1\varphi_2}] & e^{-i\lambda_1\varphi_2} + \rho^2 e^{i\lambda_2\varphi_2} \end{pmatrix}. \tag{45}$$

From Eq.(38), we find that $S(k_{so}, q)$ becomes a function of θ_{so} and is given by

$$S(\theta_{so}) = \frac{1}{2\cos(\lambda_1\pi)}[S_1(\pi) + S_2(\pi)], \tag{46}$$

$$= \exp(i\delta\sigma_2), \tag{47}$$

with $\delta = \arctan(2\theta_{so})$. Compare Eq.(46) to (38), we find that the function $f(k_{so}, q)$ also becomes a function of θ_{so} and is given by $f(\theta_{so}) = 4\cos^2(\lambda_1\pi) = 4\cos^2(\Phi_{AC}/2)$ with the Aharonov-Casher phase defined as $\Phi_{AC} \equiv \pi[\sqrt{1+4\theta_{so}^2} - 1]$.

Take the above results into Eq.(40) and (41), we find the transfer matrix for the ring scatterer

$$\begin{pmatrix} A_{II} \\ B_{II} \end{pmatrix} = \begin{pmatrix} t_2 & -it_1 \\ it_1 & t_2^* \end{pmatrix} \begin{pmatrix} S(\theta_{so})A_I \\ S(\theta_{so})B_I \end{pmatrix}, \tag{48}$$

with the matrix elements

$$t_2 = \frac{4kq\sin(2\pi qa) + i\{k^2[1 - \cos(2\pi qa)] + 4q^2[\cos(\Phi_{AC}) - \cos(2\pi qa)]\}}{8kq\sin(\pi qa)\cos(\Phi_{AC}/2)}, \tag{49}$$

$$t_1 = \frac{k^2[1 - \cos(2\pi qa)] - 4q^2[\cos(\Phi_{AC}) - \cos(2\pi qa)]}{8kq\sin(\pi qa)\cos(\Phi_{AC}/2)}. \tag{50}$$

Comparing Eq.(48) to Eq.(2), the parameter $\sinh\theta = t_1$ is easily read off and the criterion function is found as

$$(\cosh\theta\cos\beta)^2 = \frac{\cos^2(\pi qa)}{\cos^2(\Phi_{AC}/2)}. \tag{51}$$

From Eq.(51), electron localization will occur at some specific values of the spin-orbit coupling, $\theta_{so} = \sqrt{4n^2 - 1}/2$ for all integers $n \neq 0$, for a linear chain of the ring scatterers in the large N limit.

D. Circular loops in the presence of a perpendicular magnetic field

Consider the same circular loop in the presence of a perpendicular magnetic field $\vec{B} = B\hat{z}$ but without the spin-orbit interaction. The electron wave functions in the two leads are given in Eq.(15) and (16). From the results in Eq.(19), (20), (21), and (22), we find the transfer matrix for the ring scatterer

$$\begin{pmatrix} A_{II} \\ B_{II} \end{pmatrix} = \begin{pmatrix} t_2 & -it_1 \\ it_1 & t_2^* \end{pmatrix} \begin{pmatrix} A_I \\ B_I \end{pmatrix}, \tag{52}$$

with

$$t_2 = \frac{4\sin(2\pi ka) + i[1 - 5\cos(2\pi ka) + 4\cos(\Phi_{AB})]}{8\sin(\pi ka)\cos(\Phi_{AB}/2)}, \tag{53}$$

$$t_1 = \frac{1 + 3\cos(2\pi ka) - 4\cos(\Phi_{AB})}{8\sin(\pi ka)\cos(\Phi_{AB}/2)}. \tag{54}$$

Here $\Phi_{AB} \equiv e\pi a^2 B/\hbar$ denotes the Aharonov-Bohm flux in the ring. From Eq.(54) and (53), we read off the parameter $\sinh\theta = t_1$ and the criterion function for the chain of rings is given in Eq.(14). From Eq.(14) we know that electron localization will occur for $\Phi_{AB} = (2n+1)\pi$ for all integers n.

E. square loops with spin-orbit interaction

Consider that an electron with energy $\varepsilon = \hbar^2 k^2/2m$ is injected to the linear chain of square loops as shown in Fig.6. The length of each side of the squares is denoted as ℓ. Therefore both the lengths of the upper arm and the lower arm are equal $L_1 = L_2 = 2\ell$. As discussed in literature[8], electron localization will occur in the square loop chain with the spin-orbit interaction. In this paper, we obtain the same results by using the formulas given in the previous subsections.

From Eq.(29) and (30), we find the total spin-rotation operators for the upper and the lower arms of a square loop to be

$$S_1 = e^{i\theta_{so}\sigma_+} e^{i\theta_{so}\sigma_-}, \tag{55}$$

$$S_2 = e^{i\theta_{so}\sigma_-} e^{i\theta_{so}\sigma_+}, \tag{56}$$

where $\sigma_\pm \equiv \frac{1}{\sqrt{2}}(\sigma_2 \pm \sigma_1)$, and θ_{so} is defined as $\theta_{so} = k_{so}\ell$. The function $f(k_{so}, q)$ in Eq.(39) thus becomes a function of θ_{so}, $f(\theta_{so}) = 4\cos^2\theta_{so}(1 + \sin^2\theta_{so})$.

From Eq.(37), we find the transfer matrix for the square loop

$$\begin{pmatrix} A_{II} \\ B_{II} \end{pmatrix} = \begin{pmatrix} t_2 & -it_1 \\ it_1 & t_2^* \end{pmatrix} \begin{pmatrix} S(\theta_{so})A_I \\ S(\theta_{so})B_I \end{pmatrix}, \tag{57}$$

where t_2 and t_1 are obtained from Eq.(40) and (41) by taking $\theta_1 = \theta_2 = 2q\ell \equiv 2\theta_q$

$$t_2 = \frac{2\cos(2\theta_q)}{\sqrt{f(\theta_{so})}} + i\left\{\frac{k^2\sin^2(2\theta_q) + q^2[f(\theta_{so}) - 4\cos^2(2\theta_q)]}{2kq\sin(2\theta_q)\sqrt{f(\theta_{so})}}\right\}, \tag{58}$$

$$t_1 = \frac{k^2\sin^2(2\theta_q) - q^2[f(\theta_{so}) - 4\cos^2(2\theta_q)]}{2kq\sin(2\theta_q)\sqrt{f(\theta_{so})}}, \tag{59}$$

with $q = \sqrt{k^2 + k_{so}^2}$. The matrix $S(\theta_{so})$ is obtained from Eq.(38)

$$S(\theta_{so}) \equiv \frac{1}{\sqrt{f(\theta_{so})}} \begin{pmatrix} 2\cos^2\theta_{so} & \sqrt{2}\sin(2\theta_{so}) \\ -\sqrt{2}\sin(2\theta_{so}) & 2\cos^2\theta_{so} \end{pmatrix}. \tag{60}$$

It is noted that $S(\theta_{so})$ is unitary. Once again, the transfer matrix in Eq.(57) is of the type $T \otimes S$. The parameter $\sinh\theta$ in Eq.(2) is then easily read off by $\sinh\theta = t_1$, and the criterion function for the square loop scatterer is found by

$$(\cosh\theta\cos\beta)^2 = \frac{4\cos^2(2\theta_q)}{f(\theta_{so})}. \tag{61}$$

In this case, electron localization occurs at $f(\theta_{so}) = 0$, i.e., $k_{so}\ell = (n + 1/2)\pi$ for all integers n.

F. square loops in the presence of a magnetic field

Consider the same square loop in the presence of a perpendicular magnetic field $\vec{B} = B\hat{z}$ but without the spin-orbit interaction. The electron wave functions in the two leads are given in Eq.(15) and (16). From the results in Eq.(19),

(20), (21), and (22), we find the transfer matrix for the square loop scatterer

$$\begin{pmatrix} A_{II} \\ B_{II} \end{pmatrix} = \begin{pmatrix} t_2 & -it_1 \\ it_1 & t_2^* \end{pmatrix} \begin{pmatrix} A_I \\ B_I \end{pmatrix},$$ (62)

with

$$t_2 = \frac{4\sin(4\theta_k) + i[1 - 5\cos(4\theta_k) + 4\cos(\Phi_{AB})]}{8\sin(2\theta_k)\cos(\Phi_{AB}/2)},$$ (63)

$$t_1 = \frac{1 + 3\cos(4\theta_k) - 4\cos(\Phi_{AB})}{8\sin(2\theta_k)\cos(\Phi_{AB}/2)}.$$ (64)

Here $\theta_k \equiv k\ell$, and $\Phi_{AB} \equiv eB\ell^2/\hbar$ denotes the Aharonov-Bohm flux in the square loop. From Eq.(63) and (64), we read off the parameter $\sinh\theta = t_1$ and the criterion function for the square loop chain

$$(\cosh\theta\cos\beta)^2 = \frac{\cos^2(2\theta_k)}{\cos^2(\Phi_{AB}/2)}.$$ (65)

Obviously, electron localization will occur for $\Phi_{AB} = (2n+1)\pi$ for all integers n.

G. triangular loops in the presence of a magnetic field

In this subsection, we discuss the effect of unequal arm lengths by considering the triangular loop chain in the presence of a perpendicular magnetic field B as shown in Fig.7. Each side of the triangle has the same length ℓ. Therefore the length of the upper arm is twice the length of the lower arm, $L_1 = 2L_2 = 2\ell$. Similar to the square loop chain discussed in the paper, the triangular loop chain also possesses bipartite structure containing nodes with different coordination numbers. The lattice nodes have either coordination number 2 or coordination number 4. However, unlike the square loop chain, the triangular loop chain has no electron localization even in the presence of a perpendicular magnetic field.

Once again, the wave functions in the two leads are given in Eq.(15) and (16). By defining the Aharonov-Bohm flux $\Phi_{AB} = \sqrt{3}eB\ell^2/4\hbar$ and the phase $\theta_k = k\ell$, we obtain the transfer matrix for the triangular loop from Eq.(19), (20), (21) and (22) by

$$\begin{pmatrix} A_{II} \\ B_{II} \end{pmatrix} = e^{i\alpha} \begin{pmatrix} t_2 & -it_1 \\ it_1 & t_2^* \end{pmatrix} \begin{pmatrix} A_I \\ B_I \end{pmatrix},$$ (66)

where the phase α is a function of Φ_{AB} and θ_k, $\alpha = \arctan[\sin\Phi_{AB}/(2\cos\theta_k + \cos\Phi_{AB})]$. The parameters t_1 and t_2 are given by

$$t_2 = \frac{4\sin(3\theta_k) + i[\cos\theta_k - 5\cos(3\theta_k) + 4\cos\Phi_{AB}]}{4\sin\theta_k\sqrt{1 + 4\cos^2\theta_k + 4\cos\theta_k\cos\Phi_{AB}}},$$ (67)

$$t_1 = \frac{\cos\theta_k + 3\cos(3\theta_k) - 4\cos\Phi_{AB}}{4\sin\theta_k\sqrt{1 + 4\cos^2\theta_k + 4\cos\theta_k\cos\Phi_{AB}}}.$$ (68)

We then read off the parameter $\sinh\theta = t_1$ and the criterion function for a chain of N identical triangular loops in the large N limit from Eq.(67) and (68).

$$(\cos\beta\cosh\theta)^2 = \frac{(4\cos^2\theta_k - 1)^2}{1 + 4\cos^2\theta_k + 4\cos\theta_k\cos\Phi_{AB}}.$$ (69)

From the criterion function, we know that no electron localization will occur since no values of Φ_{AB} could always satisfy the condition that $(\cos\beta\cosh\theta)^2 > 1$ for all θ_k values.

H. triangular loops with spin-orbit interaction

The last example studied is the same triangular loop chain with only the spin-orbit interaction. The electrons are injected into the chain with energy $\varepsilon = \hbar^2 k^2/2m$. From Eq.(29) and (30), the total spin-rotation operators for the upper arm and the lower arm are

$$S_1 = e^{i\theta_{so}\sigma_{23}} e^{i\theta_{so}\sigma_{12}},$$ (70)

$$S_2 = e^{i\theta_{so}\sigma_2}.$$ (71)

Here σ_{12} and σ_{32} are defined as $\sigma_{12} \equiv (-\frac{\sqrt{3}}{2}\sigma_1 + \frac{1}{2}\sigma_2)$ and $\sigma_{23} \equiv (\frac{\sqrt{3}}{2}\sigma_1 + \frac{1}{2}\sigma_2)$, and $\theta_{so} \equiv k_{so}\ell$.

From Eq.(37), we obtain the transfer matrix for the triangular loop scatterer

$$\begin{pmatrix} A_{II} \\ B_{II} \end{pmatrix} = \begin{pmatrix} t_2 & -it_1 \\ it_1 & t_2^* \end{pmatrix} \begin{pmatrix} S(k_{so}, q)A_I \\ S(k_{so}, q)B_I \end{pmatrix}, \tag{72}$$

where t_1 and t_2 are obtained from Eq.(40) and (41) as

$$t_2 = \frac{3 - 4\sin^2\theta_q}{\sqrt{f(k_{so}, q)}} + i\{\frac{k^2\sin^2(2\theta_q) + q^2[f(k_{so}, q) - (3 - 4\sin^2\theta_q)^2]}{2kq\sin(2\theta_q)\sqrt{f(k_{so}, q)}}\}, \tag{73}$$

$$t_1 = \frac{k^2\sin^2(2\theta_q) - q^2[f(k_{so}, q) - (3 - 4\sin^2\theta_q)^2]}{2kq\sin(2\theta_q)\sqrt{f(k_{so}, q)}}, \tag{74}$$

where $q = \sqrt{k^2 + k_{so}^2}$ and $\theta_q \equiv q\ell$. Here $f(k_{so}, q)$ is obtained from Eq.(39) by $f(k_{so}, q) = 1 + 4\cos^2\theta_q + 2\cos\theta_q(3\cos\theta_{so} - \cos^3\theta_{so})$. It is noted that $f(k_{so}, q) \geq 0$ is always held for all θ_{so} and θ_q. The unitary matrix $S(k_{so}, q)$ is acting on the spinor amplitudes (A_I, B_I) and is defined as $S(k_{so}, q) \equiv (S_1 + 2\cos\theta_q S_2)/\sqrt{f(k_{so}, q)}$.

Eq.(72) shows that the transfer matrix for the triangular loop scatterer is of the type $T \otimes S$. Therefore, the conductance of the loop chain is merely determined by T, the spatial part of the transfer matrix. From Eq.(72), we easily read off the parameter $\sinh\theta = t_1$ and the criterion function

$$(\cos\beta\cosh\theta)^2 = \frac{(3 - 4\sin^2\theta_q)^2}{f(k_{so}, q)}. \tag{75}$$

Obviously, electron localization will not occur in the triangular loop chain since the zero-transmission condition $(\cos\beta\cosh\theta)^2 > 1$ will not hold for all k values with any specific value of θ_{so}.

IV. AVERAGED TRANSMISSION PROBABILITIES

In this section we present the method of integrating the transmission probability over the injection wave vector k for the linear loop chains discussed in the paper. Throughout the paper, the averaged transmission probability will be indicated by $\langle P \rangle_k$. It is known that finite temperature or finite voltage will introduce an average over k in a natural way[8,9].

To integrate the transmission probability over k we need not only the knowledge of the criterion function but also the parameter $\sinh\theta$ as indicated in section III. We have to find the criterion function and $\sinh\theta$ as functions of the wave vector k and other physical factors. The expression for the integrated transmission probability is thus derived in the integral form. In the numerical calculation, we take the approximation $q \approx k$. It can be understood as follows. Taking for the Fermi energy of the single-channel wires 10 meV, the loop radius a or the arm length $L \sim a \sim 0.25$ μm, and $m/m_e = 0.042$ for the effective mass of InAs, yields $k_F a \sim k_F L \sim 26$. Therefore we could replace qa by ka in the criterion function in the situation that $k_{so}a \sim k_{so}L \sim \mathcal{O}(1)$.

In this section we calculate the averaged transmission probabilities for the loop chains discussed in section III. As shown in Fig.8, we find that the plots of the averaged transmission probabilities resemble each other for the square and the circular loop chains. Though the shapes of the loops as well as the physical effects present in the chains may be different from each other, the square chains and the circular chains do have something in common. They all have their loops be annexed at the nodes that equally divide the loops into upper arms and lower arms with equal arm lengths. The last linear chain discussed in the section is the triangular loop chain as shown in Fig.7. The length of the upper arm is twice the length of the lower arm in the triangular loop. The plots of the averaged transmission probability are quite different for the chain, as compared to the plots for the square and the circular loop chains. Besides, no electron localization will occur in the chain. The results suggest that electron localization may not have much to do with the bipartite structure of the lattice nodes containing different coordination numbers. Instead, it has strong ties with the arm lengths of the loop scatterers. As suggested by the results, electron localization is more likely to occur in the linear loop chains that have equal arms in the loops.

A. square loop chain with spin-orbit effects

The first example is a linear chain of N square loops in the the presence of the spin-orbit interaction in the large N limit. In the numerical calculation, we replace the wave vector q with the injection wave vector k. From

Eq.(61), the criterion function is $(\cosh\theta\cos\beta)^2 = 4\cos^2(2\theta_k)/f(\theta_{so})$. Non-vanishing electronic transmission occurs at $(\cosh\theta\cos\beta)^2 \leq 1$. Therefore for a given θ_{so}, non-vanishing transmission occurs at $2M\pi + \theta_0 \leq 2\theta_k \leq (2M+1)\pi - \theta_0$ with $\theta_0 \equiv \arccos[\sqrt{1 - \sin^4\theta_{so}}]$ in the range $2\theta_k \in [2M\pi, (2M+1)\pi]$ for integer M. In the non-vanishing transmission scenario, we define the variable Ω by $\cos\Omega \equiv \cos(2\theta_k)/\cos\theta_0$. From Eq.(13), the averaged transmission probability $\langle P \rangle_k$ as a function of θ_{so} is thus given by integrating $|t^2|$ over $2\theta_k$

$$\langle P \rangle_k = \frac{1}{\pi}\int_{\theta_0}^{\pi-\theta_0} \frac{\sin\Omega}{\sqrt{\sin^2\Omega + \sinh^2\theta}}d(2\theta_k). \tag{76}$$

The parameter $\sinh^2\theta$ is obtained from Eq.(59) as

$$\sinh^2\theta = \frac{[1 + \cos^2\theta_0(3\cos^2\Omega - 4)]^2}{16\cos^2\theta_0(1 - \cos^2\theta_0\cos^2\Omega)}. \tag{77}$$

Finally, we obtain the integrated transmission probability in the integral form

$$\langle P \rangle_k = \frac{\cos\theta_0}{\pi}\int_0^{\pi} \frac{\sin^2\Omega d\Omega}{\sqrt{1 - \cos^2\theta_0\cos^2\Omega}\sqrt{\sin^2\Omega + \sinh^2\theta}}. \tag{78}$$

Obviously, $\langle P \rangle_k$ is invariant under the transformations $\theta_{so} \to \theta_{so} + \pi$ and $\theta_{so} \to \pi - \theta_{so}$. The averaged transmission probability as a function of (θ_{so}/π) is plotted in Fig.8. $\langle P \rangle_k$ has its maximum value at $(\theta_{so}/\pi) = 0$ and decreases as (θ_{so}/π) approaching $1/2$. Electron localization occurs at $(\theta_{so}/\pi) = 1/2$, consistent with the prediction derived from the criterion function.

B. square loop chain in the presence of a perpendicular magnetic field

The second example is the same linear chain of square loops in the presence of a perpendicular magnetic field B. No spin-orbit interaction is assumed to present in the loops. For this example, the criterion function for electron transmission is given in Eq.(65). The non-vanishing transmission scenarios occur at $\pi - \theta_0 \geq 2\theta_k \geq \theta_0$, with $\theta_0 \equiv \arccos[|\cos(\Phi_{AB}/2)|]$. By defining $\cos\Omega = \cos(2\theta_k)/\cos\theta_0$, we find the parameter $\sinh^2\theta$ has the same expression as that in Eq.(77). The integrated transmission probability $\langle P \rangle_k$ is also found to have the same expression as given in Eq.(78). The averaged transmission probability as a function of (Φ_{AB}/π) is also plotted in Fig.8. As shown in the figure, the plot is a bit different to the plot given in the previous example. $\langle P \rangle_k$ also has its maximum value at $(\Phi_{AB}/\pi) = 0$, and decreases as (Φ_{AB}/π) approaching $1/2$. In this case, electron localization occurs at $(\Phi_{AB}/\pi) = 1/2$.

C. circular loop chain in the presence of a perpendicular magnetic field

The third example is the chain of circular loops in the presence of a perpendicular magnetic field as described in section III. The criterion function for the chain is given in Eq.(14) and the parameter $\sinh\theta$ appeared in the transfer matrix T is equal to the parameter t_1 in Eq.(54). Both the criterion function and $\sinh^2\theta$ are periodic function of k.

From Eq.(14), we find the criterion function is no larger than 1 for $(1 - \theta_o/\pi) \geq ka \geq \theta_0/\pi$ in the range $ka \in [0, 1]$ with $\theta_o \equiv \arccos(|\cos(\Phi_{AB}/2)|)$. By defining $\cos\Omega \equiv \cos(\pi ka)/\cos(\theta_0)$, the expression of the parameter $\sinh^2\theta$ is also given in Eq.(77). The integrated transmission probability $\langle P \rangle_k$ is found to have the same expression as given in Eq.(78). The averaged transmission probability as a function of (Φ_{AB}/π) is also plotted in Fig.8. In fact, the plot is identical to the plot in the previous example.

D. circular loop chain with spin-orbit effects

The forth example is the chain of circular loops with the spin-orbit interaction in the absence of the magnetic field. The criterion function as well we the parameter $\sinh\theta$ are given in Eq.(51) and (50), respectively. Here we replace qa with ka in both the criterion function and in the expression of t_1. Thus we find the criterion function is no larger than 1 for $2M\pi + \theta_0 \leq \pi ka \leq (2M+1)\pi - \theta_0$ for integer M with $\theta_0 \equiv \arccos[|\cos(\Phi_{AC}/2)|]$. By defining $\cos\Omega = \cos(\pi ka)/\cos(\theta_0)$, we find that the parameter $\sinh^2\theta$ is also given in Eq.(77) and the integrated transmission probability $\langle P \rangle_k$ is also found to have the same expression as given in Eq.(78). The averaged transmission probability as a function of (Φ_{AC}/π) is plotted in Fig.8. Once again, the plot for the averaged transmission probability is identical to the plots in the previous two examples.

E.   triangular loop chain in the presence of a perpendicular magnetic field

The fifth example is the chain of triangular loops in the presence of a perpendicular magnetic field as described in section III. The criterion function $(\cos \beta \cosh \theta)^2$ as well as the parameter $\sinh \theta$ can be found in Eq.(69) and (68), respectively. Obviously, both the criterion function and $\sinh \theta$ are periodic functions of both the wave vector k and the Aharonov-Bohm flux Φ_{AB}. Therefore we will integrate the transmission probability over θ_k in the range $\theta_k \in [0, \pi]$,

$$\langle P \rangle_k = \frac{1}{\pi} \int_0^\pi \Theta[1 - \cos^2 \beta \cosh^2 \theta] \{ \frac{1 - \cos^2 \beta \cosh^2 \theta}{1 - \cos^2 \beta \cosh^2 \theta + \sinh^2 \theta} \}^{1/2} d\theta_k. \tag{79}$$

Here $\Theta[1 - \cos^2 \beta \cosh^2 \theta]$ denotes the step function that equals 1 for $1 \geq \cos^2 \beta \cosh^2 \theta$ and vanishes otherwise. The averaged transmission probability as a function of Φ_{AB}/π is also plotted in the range $(\Phi_{AB}/\pi) \in [0, 1]$ as shown in Fig.8. Different to the previous four examples in this section, there is no electron localization in the chain of triangular loops. Besides, $\langle P \rangle_k$ increases as (Φ_{AB}/π) approaching $1/2$. Once again, the absence of electron localization is also seen from the criterion function in Eq.(69).

F.   triangular loop chain with spin-orbit interaction

The last example that we consider is the same triangular loop chain but in the presence of only the spin-orbit effect. Once again, we replace q by k in the numerical calculation thus $\theta_q = \theta_k$. The criterion function and the parameter $\sinh \theta$ are given in Eq.(75) and (74), respectively. Similarly, they are periodic functions of θ_k and θ_{so}. Therefore we will also integrate the transmission probability over θ_k in the range $\theta_k \in [0, \pi]$. The integral formula for the averaged transmission probability $\langle P \rangle_k$ is also given in Eq.(79). Obviously, $\langle P \rangle_k$ is now a function of θ_{so}. $\langle P \rangle_k$ as a function of θ_{so}/π is also plotted in Fig.8. Once again, the plot shows no electron localization in the chain. This conclusion can also be easily drawn from the criterion function given in Eq.(75). As shown in the figure, the plot of $\langle P \rangle_k$ in this case is similar to the plot for the same triangular loop chain in the presence of a perpendicular magnetic field. In fact, the plots of $\langle P \rangle_k$ for the square and the circular loop chains also resemble each other even though the chains may have different effects such as the spin-orbit effect or the Aharonov-Bohm effect. This observation is quite interesting and seems to be generic for various kinds of the loop chains. Both the Aharonov-Bohm effect and the spin-orbit effect may lead to similar behaviors in the averaged conductances for the linear chains of similar loop structures. Here we think of the square loop chain and the circular loop chain discussed in the paper to have similar loop structure, since the annex nodes of a loop in the chains equally divide the loop into two arms of equal lengths.

V.   CONCLUSION

In this paper we discussed the integrated transmission probability over the wave vector k for electrons moving in the linear chains of identical loop scatterers, in the presence of either the spin-orbit interaction or a perpendicular magnetic field. We showed that the averaged transmission probability is only determined by some parameters of the transfer matrix of a single loop scatterer, and can be easily calculated from the knowledge of the parameters. In fact, the presence or the absence of electron localization in a linear chain of identical scatterers is easily known from the square of the real part of one of the transfer matrix elements, called the criterion function in this paper, of a single loop scatterer.

The results also show that electron localization is due to the interplay of the loop geometry and the physical effects such as the applied magnetic field or the spin-orbit interaction. The loop geometry plays an important role in the localization phenomenon. For example, electron localization is found to present in the linear chains of identical loops with equal arms. This is due to the fact that totally destructive interference of electronic waves is more likely to happen in the equal-arm loops. It is understood in the following ways. Consider an equal-arm loop scatterer in the presence of a perpendicular magnetic field. The arm length of the loop is denoted as L. An electron will acquire an Aharonov-Bohm phase Φ_1 along with a phase kL when travelling in the upper arm of the loop. The electron will also acquire an Aharonov-Bohm phase Φ_2 along with the same phase kL when travelling in the lower arm of the loop. Total destruction of electronic waves at the output lead thus occurs when $e^{i(kL+\Phi_1)} + e^{i(kL+\Phi_2)} = 0$ is satisfied, or equivalently for $\Phi_{AB} \equiv \Phi_1 - \Phi_2 = (2n+1)\pi$ no matter what the value of k is. The total destruction of waves still survives even after integrating out the wave vector k. Therefore electron localization will occur at the specific values of Φ_{AB}. Similarly, electron localization in the equal-arm loop chains in the presence of the spin-orbit interaction can also be understood in the same way. When an electron is moving in the upper arm of the loop, the electron spinor will acquire a phase kL and be rotated by the spin-rotation operator S_1. When an electron is moving in the lower

arm of the loop, the electron spinor will also acquire a phase kL and be rotated by the spin-rotation operator S_2. Here S_1 and S_2 depend on only the loop geometry and the strength of the spin-orbit interaction. Total destruction of electronic waves thus occurs when $(e^{ikL}S_1 + e^{ikL}S_2) = 0$ is satisfied, or equivalently $\sqrt{2[1 + \cos(\Theta_{so})]}e^{ikL}S(k_{so}) = 0$ with $\cos(\Theta_{so}) = \frac{1}{4}\mathtt{Tr}(S_1 S_2^{-1} + S_2 S_1^{-1})$. Therefore electron localization will occur in the chain of equal-arm loops for $\cos\Theta_{so} = -1$.

The resemblance between the plots of the averaged transmission probabilities can be explained as follows. As pointed in section II, the transmission probability of a loop chain is totally determined by the transfer matrix of a single loop scatterer. The current conservation along with the single-channel assumption for the quantum wires thus put strong restrictions on the possible forms of the transfer matrix. Furthermore, both the Aharonov-Bohm effect and the Aharonov-Casher effect play similar roles in the electronic transmission problem. Electrons travelling in the arms of the loops can acquire additional quantum phases due to either the Aharonov-Bohm effect or the Aharonov-Casher effect. Therefore, the transfer matrices for the loop scatterers discussed in the paper also resemble each other. The resemblance between the transfer matrices thus leads to the resemblance between the plots of the averaged transmission probabilities.

[*] Electronic address: choucl@cycu.edu.tw

[1] J. Vidal, R. Mosseri, and B. Douçot, Phys. Rev. Lett. **81**, 5888 (1998).

[2] Y. Aharonov and D. Bohm, Phys. Rev. **115**, 485 (1959).

[3] C. C. A. *et al.*, Phys. Rev. Lett. **83**, 5102 (1999).

[4] C. Naud, G. Faini, and D. Mailly, Phys. Rev. Lett. **86**, 5104 (2001).

[5] J. Vidal, P. Butaud, B. Douçot, and R. Mosseri, Phys. Rev. B **64**, 155306 (2001).

[6] J. Vidal, B. Douçot, R. Mosseri, and P. Butaud, Phys. Rev. Lett. **85**, 3906 (2000).

[7] J. Vidal, G. Montambaux, and B. Douçot, Phys. Rev. B **62**, R16294 (2000).

[8] D. Bercioux, M. Governale, V. Cataudella, and V. M. Ramaglia, Phys. Rev. Lett. **93**, 056802 (2004).

[9] D. Bercioux, M. Governale, V. Cataudella, and V. M. Ramaglia, Phys. Rev. B. **72**, 075305 (2005).

[10] Y. Aharonov and A. Casher, Phys. Rev. Lett. **53**, 319 (1984).

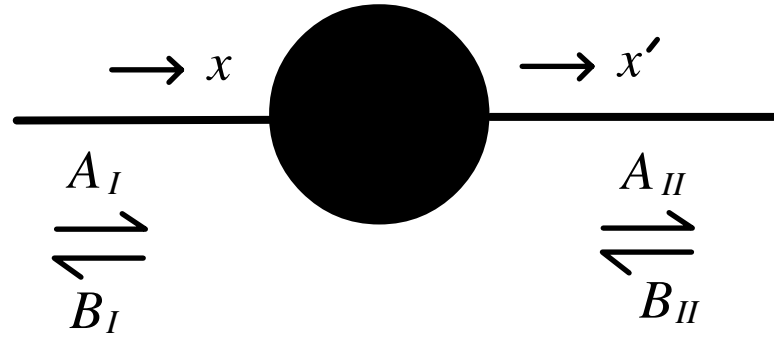[11] B. Molnár, P. Vasilopoulos, and F. M. Peeters, Phys. Rev. B. **72**, 075330 (2005).

FIG. 1: Single-channel scatterer with A_I, B_{II} and A_{II}, B_I being the amplitudes of the incoming and the outgoing electronic waves, respectively. The dark circle represents the scatterer.
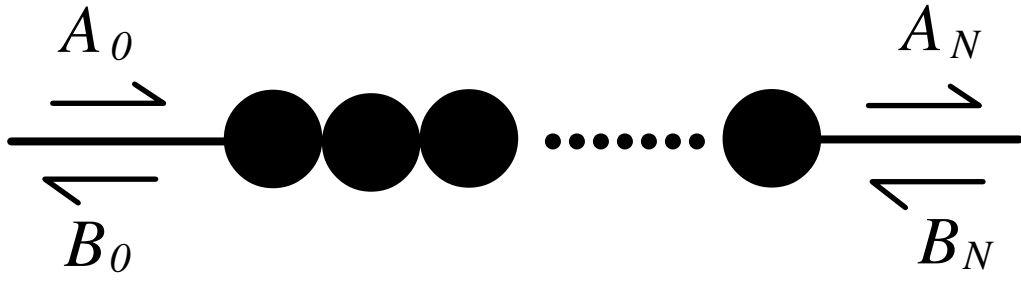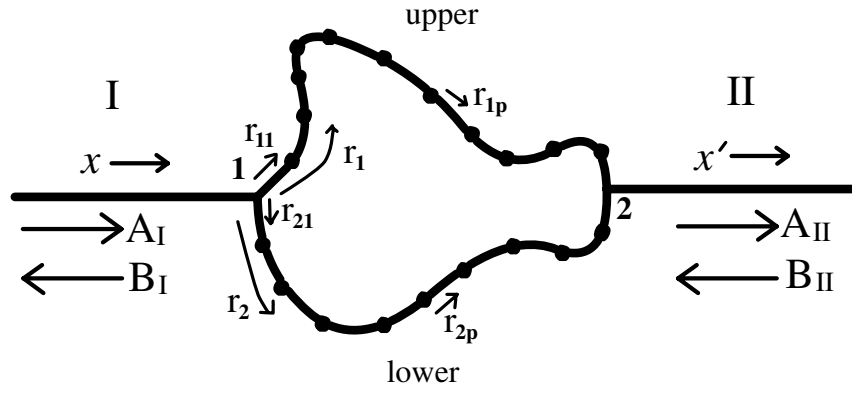
FIG. 2: A chain of N identical scatterers.
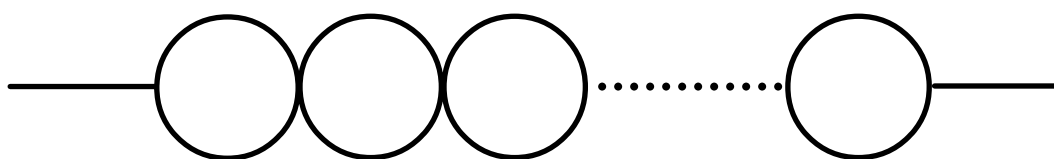
FIG. 3: A simple loop with two attached leads.
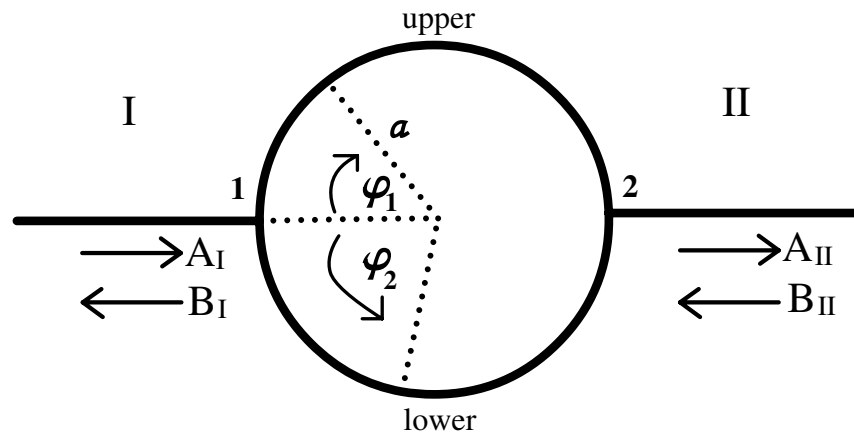
FIG. 4: A chain of N identical rings.

FIG. 5: A single ring with two attached leads.

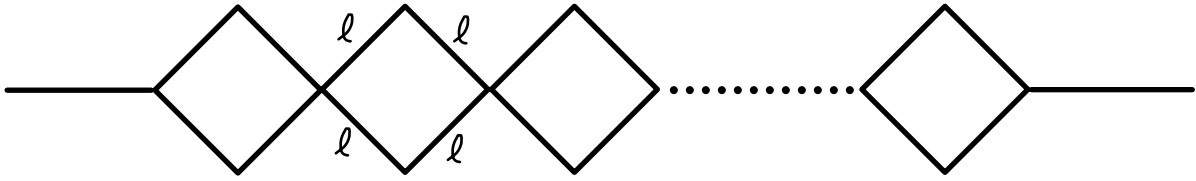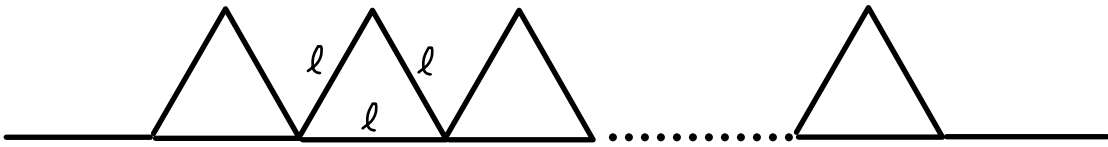FIG. 6: A chain of N identical square loops.

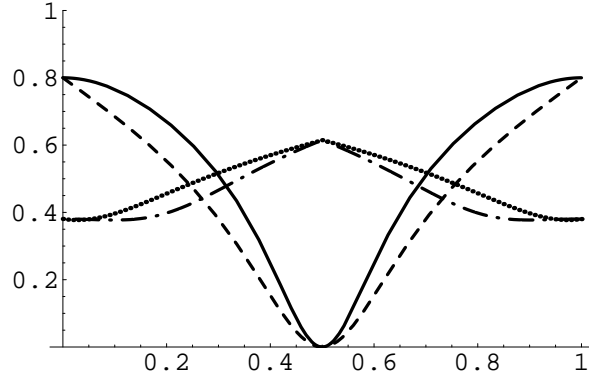FIG. 7: A chain of N identical triangular loops.

FIG. 8: The integrated transmission probability $\langle P \rangle_k$ over the injection wave vector k for the linear chains of N identical loop scatterers in the large N limit. Solid line represents $\langle P \rangle_k$ as a function of $(k_{so}\ell/\pi)$ in the presence of the spin-orbit interaction for the square loop chain. Doted line and dot-dashed line represent $\langle P \rangle_k$ as functions of Φ_{AB}/π and $k_{so}\ell/\pi$ for the triangular loop chain in the presence of either a perpendicular magnetic field or the spin-orbit effect, respectively. Dashed line represents $\langle P \rangle_k$ for (a) the square loop chain in the presence of a perpendicular magnetic field as a function of (Φ_{AB}/π), and for (b) the circular loop chain in the presence of either a perpendicular magnetic field or the spin-orbit interaction as the function of (Φ_{AB}/π) or (Φ_{AC}/π), respectively.